Algal Reactor Design Based on Comprehensive Modeling of Light and Mixing

Alexandra D. Holland and Joseph M. Dragavon

Abstract The prospect of autotrophic (or light-driven) algal biomass production as a sustainable substitute for fossil feedstocks has yet to fulfill its potential. As a likely cause, the inability to robustly account for algal biomass production rates has prevented the derivation of satisfactory mass balances for the simple parameterization of bioreactors. The methodology presented here aims at resolving this shortcoming. Treating photons as a substrate continuously fed to algae provides the grounds to define an autotrophic yield Φ^{DW}, in grams of dry weight per mole of photons absorbed, as an operating parameter. Under low irradiances, the rate of algal biomass synthesis is the product of the yield Φ^{DW} and the flux of photons absorbed by the culture, modeled using a scatter-corrected polychromatic Beer-Lambert law. This work addresses the broad misconception that Photosynthesis-Irradiance curves, or the equivalent use of specific growth rate expressions independent of the biomass concentration, can be extended to adequately model biomass production under light-limitation. Since low photon fluxes per cell maximize Φ^{DW}, the photosynthetic units mechanistic model was adapted to determine a corresponding maximum residence time under high light. Such high speeds in the photic zone, which call for fundamental changes in bioreactor design, enable the use of Φ^{DW} to describe biomass productivity under otherwise inhibitory irradiances. Nitrogen limitation-induced lipid accumulation corresponds to a photon flux excess with respect to the rate of nitrogen uptake, such that continuous lipid production can be achieved using the Φ^{DW} and nitrogen quotient parameters. Additionally, energy to photon-counts conversion factors are derived.

Keywords Algal chemostat parameterization · Algal growth autotrophic yield · Continuous algal lipid production · Photic zone target speed · Photosynthetic units mechanistic model · Scatter-corrected polychromatic Beer-Lambert law

A. D. Holland (✉)
2 Les Létumières, 61190, Moussonvilliers, France
e-mail: alex@piarc-solutions.com

R. Bajpai et al. (eds.), *Algal Biorefineries,* DOI 10.1007/978-94-007-7494-0_2,

Abbreviations and Nomeclature

A. Abbreviations

AM	Air-mass
AU	Absorbance unit
CARPT	Computer-automated radioactive particle tracking
Chl *a*	Chlorophyll *a*
DW	Dry weight
ELT	Exponential-to-linear
LHS	Left hand side
NPQ	Non-photochemical quenching
NREL	National Renewable Energy Laboratory
PAR	Photosynthetically active radiation (400-700 nm)
PI	Photosynthesis-irradiance
PPFD	Photosynthesis photon flux density
PQ	Plastoquinone
PSI	Photosystem I
PSII	Photosystem II
PSU	Photosynthetic unit
REC	Reduced carrier
Q_A	Quinone A
SC	Scatter-corrected

B. Variables and Corresponding Units

a [mol_{PSII}]	Number of open of PSII centers (or oxidized)
a^* [mol_{PSII}]	Number of closed of PSII centers (or reduced)
a_0 [mol_{PSII}]	Total number of PSII centers
$Abs_{RAW}(\lambda)$ [AU]	Raw algal absorption at wavelength λ
$Abs_{SC}(\lambda)$ [AU]	Scatter-corrected algal absorption at wavelength λ
$Abs_{SCATTER}(\lambda)$ [AU]	Scatter contribution to algal absorption at wavelength λ
A_C [m^2]	Area of the culture perpendicular to the light source
C [$g_{DW}\ m^{-3}$]	Algal culture biomass concentration in the bioreactor
c [$m\ s^{-1}$]	Celerity of light
C_0 [$g_{DW}\ m^{-3}$]	Algal culture biomass concentration at inoculation time t_0
C_E, [$g_{DW}\ m^{-3}$]	Culture biomass concentration during spectrum acquisition
c_{EJ} [$E\ J^{-1}$]	Einstein-to-Joules conversion factor
C_{PI} [$g_{DW}\ m^{-3}$]	Algal biomass concentration in the PI chamber
d [m]	Depth of the photic zone, where light is $>99\%\ I_0$
$E_P(\lambda)$ [$W\ m^{-2}\ nm^{-1}$]	Photon energy reported for each wavelength increment $d\lambda$
$EF(x)$ μE $g_{DW}^{-1}\ h^{-1}$	Specific energy flux at depth x
EF_T μE $g_{DW}^{-1}\ h^{-1}$	Threshold specific energy flux at onset of light limitation
$E_{LIGHT}(\lambda)$ [counts nm^{-1}]	Light source emission spectrum at λ
F_{CHEM} [$m^3\ h^{-1}$]	Chemostat volumetric flow rate (bioreactor)

F [$mol_{PSII}\ g_{DW}^{-1}$]	Weight fraction of PSII
F_{IN} [$m^3\ h^{-1}$]	Inlet stream volumetric flow rate (bioreactor)
F_{OUT} [$m^3\ h^{-1}$]	Outlet stream volumetric flow rate (bioreactor)
F_{PAR} [-]	Fraction of energy in the PAR region
h [SI Units]	Planck's constant
$I(x)$ [$\mu E\ m^{-2}\ h^{-1}$]	Local PPFD at a given depth x
I_0 [$\mu E\ m^{-2}\ h^{-1}$] or [$\mu E\ m^{-2}\ s^{-1}$]	Incident photosynthesis photon flux density (PPFD)
I_{ABS} [$\mu E\ m^{-2}\ h^{-1}$]	Absorbed PPFD by the algal culture
I_H [$\mu E\ m^{-2}\ s^{-1}$]	Highest possible direct normal solar irradiance
I_{OUT} [$\mu E\ m^{-2}\ h^{-1}$]	PPFD transmitted through the algal culture
I_T [$\mu E\ m^{-2}\ s^{-1}$]	Threshold irradiance at which NPQ becomes significant
k_1 [s^{-1}]	Rate of PSII excitation
k_2 [s^{-1}]	Rate of PSII relaxation
L [m]	Depth of the culture
L_E [m]	Pathlength of the light through the spectrophotometer
L_{PI} [m]	Depth of the PI chamber
m_P [$\mu E\ g_{DW}^{-1}\ h^{-1}$]	Maintenance parameter
$\dot{n}(\lambda)$ [$E\ s^{-1}\ m^{-2}\ nm^{-1}$]	Photon flux reported for each wavelength increment $d\lambda$ at λ
Na [mol^{-1}]	Avogadro's constant
OD [AU]	Algae culture absorbance at 680 nm
P [$g_{DW}\ m^{-2}\ h^{-1}$]	Algal biomass area productivity
$P(\lambda)$ [cps]	Spectrometer reading (in counts per second)
$P_{BIOREACTOR}$ [$g_{DW}\ m^{-3}\ h^{-1}$]	Bioreactor productivity
P_i [$g_{DW}\ h^{-1}$]	Zone i contribution to the algal biomass productivity
P_i^V [$g_{DW}\ m^{-3}\ h^{-1}$]	Local volumetric biomass production rate in zone i
$P_{LIGHT}(\lambda)$ [nm^{-1}]	Normalized light-source photon fraction at λ
P_{LIPIDS} [$g_{LIPIDS}\ h^{-1}$]	Lipid productivity
P_{MAX} [$g_{DW}\ m^{-2}\ h^{-1}$]	Maximum algal biomass area productivity (light-limited)
$P_{SUN}(\lambda)$ [nm^{-1}]	Normalized solar spectrum photon fraction at λ
qL [-]	Fraction of open PSII centers
qN [-]	Fraction of closed PSII centers
Q_N [$g_N\ g_{DW}^{-1}$]	Nitrogen weight fraction (or nitrogen quotient)
S [$g_S\ m^{-3}$]	Substrate S concentration in the bioreactor
S_0 [$g_S\ m^{-3}$]	Inlet stream substrate S concentration
t [h]	Time in the light phase, truncated for duration in the dark
t [s]	Time scale for the PSU model
t_0 [h]	Reference inoculation time

u [-]	PSU model integrating factor (L or S subscript indicates linear or sinusoidal trajectory submodel respectively)
V_C [m^3]	Culture volume in bioreactor
v_T [$m\ s^{-1}$]	Target velocity in the photic zone for near maximum Φ^{PSII} (additional L or S subscript indicates linear or sinusoidal trajectory submodel respectively)
x [m]	Distance from the light incidence surface
x_T [m]	Threshold depth (onset of light limitation in poorly-mixed reactor)
$Y_{C/S}$ [$g_{DW}\ g_S^{-1}$]	Biomass yield on the substrate S
$Y_{C/N}$ [$g_{DW}\ g_N^{-1}$]	Biomass yield on nitrogen substrate
β [-]	Proportionality constant between the spectrometer count reading and the incident photon flux
λ [nm]	Wavelength
μ [h^{-1}]	Specific growth rate
μ_{MAX} [h^{-1}]	Maximum specific growth rate
σ [$m^2\ g^{DW}$–1]	Monochromatic absorption cross section
σ^{DW} [$m^2\ g_{DW}^{-1}$]	Scatter-corrected algae-specific light source-dependent absorption cross section
τ [s]	Time for the incident light to excite half the threshold PSII fraction
$\psi(\lambda)$ [$m^2\ g_{DW}\ m^{-2}$]	Hyperbolic model parameter
$\omega(\lambda)$ [$m^2\ g_{DW}^{-1}$]	Hyperbolic model parameter
Φ^{APP} [$mol_{CO2}\ E^{-1}$]	Apparent efficiency parameter in mole CO_2 fixed per mole incident photons
Φ^{CO2} [$mol_{CO2}\ E^{-1}$]	Quantum yield
Φ^{DW} [$g_{DW}\ \mu E^{-1}$]	Autotrophic yield
Φ^{C2} [$mol_{OZ}\ E^{-1}$]	Quantum yield
Φ^{PSII} [-]	Photon fraction used to excite the Q_A pool, or PSII operating efficiency

1 Introduction

The prospect of autotrophic (or light-driven) algal biomass production as a sustainable substitute for fossil feedstocks holds promise, but has yet to fulfill its potential. Arguably, the discrepancy between theoretical and achieved productivities in the field results from the lack of a working comprehensive algal growth model to guide bioreactor design. Akin to the petroleum industry in the early 50's, distillation of crude oil heavily relied on trial-and-error and was as a result very wasteful. In the mid-50's, scientific contributors such as John Prausnitz pioneered molecular thermodynamics to model the behavior of such complex chemicals mixtures (Sanders 2005). The resulting ability to predict these separation properties has revolutionized

the petroleum industry, and is the cornerstone of all petrochemical processes. The approaches introduced by Holland et al. (Holland et al. 2011; Holland and Wheeler 2011), further detailed in this chapter, hold the potential to provide such model for industrial algal biomass production processes, guiding bioreactor design and parameterization to maximize biomass and lipid productivity.

The inherent particle nature of light as a growth substrate has been broadly overlooked. Treating photons as a substrate continuously fed to algae provides the grounds to define an autotrophic yield, which is key for comparing productivities as well as parameterizing bioreactors. Indeed, within the Photosynthetically Active Radiation (PAR) region, regardless of its energy, an absorbed photon exciting the photosynthetic apparatus drives carbon fixation and therefore biomass synthesis. As such, the concept of biomass yield, reported for heterotrophic growth as biomass produced per mass of input sugar substrate, translates to its autotrophic counterpart by normalizing the biomass produced per number of input photons. The unit of choice for photon counting is the Einstein (E), or mole of photons in the PAR region.

Importantly, the goal of algal bioreactor designs is to maximize yield—not solely productivity. Sun-lit outdoor ponds require land area while artificially lit bioreactors require a primary energy source (wind power or other). Hence light is an expensive substrate that should not be wasted. Biomass productivity is the product of the autotrophic yield per absorbed photon flux. Notably, under conditions of complete absorption of the photons by the algal culture, maximum yield leads to maximum productivity (Sect. 2.1). However, the converse does not hold (Sect. 3.2). Most often, algal productivities are reported (in mass per time per volume or area) with omitted incident light levels or incomplete reactor geometries. This, in turn, precludes yield-based performance comparisons between the various characterized systems. The work presented here introduces routine determination of the algal autotrophic yield as the key parameter for setup evaluation.

Current efforts toward modeling light as a nutrient treat the algal population as a whole system, whose growth rate follows saturation kinetics (Sect. 3.2). For chemical substrates, the Monod saturation kinetics reflect that the microbial population growth rate increases with increasing concentration, and saturates when the substrate reaches a concentration greater than its uptake affinity. In chemostat bioreactors, such microbial populations reach highest productivities at high substrate concentrations supporting near maximum growth rates. For light as a substrate, Photosynthesis-Irradiance (PI) curves describe the saturation behavior of the algal population growth rate (or specific rate of biomass increase) as a function of incident light. In a given bioreactor, while productivity increases with incident light levels until light excess is reached, the biomass yield decreases. As proof, at a given biomass concentration with known cell geometry, PI curve data can be used to calculate the biomass yield (from the ratio of specific growth rate to irradiance), which shows a maximum at low irradiance. As further evidence, fluorescence response studies show highest quantum yields at low light levels (Sect. 3.1). In the authors' opinion, an apparent analogy between PI curves and Monod saturation kinetics has laid the ground for widespread misleading analyses for biomass productivity calculations as well as optimization.

Once established that highest yields are reached at low light intensity, inhibitory light levels reached at the surface of most outdoor systems can be treated using two distinct methodologies. The more widespread approach is to model cell damage and energy losses as unavoidable consequences of growth. As a contrast, the work presented here uses the same mechanistic model to derive bioreactor characteristics enabling highest yields under high irradiance. Indeed, in a dense algal culture, high speeds across the photic zone allows for high frequency light-dark fluctuations, which therefore reduce photon flux per cell to levels conducive to high yield biomass production. Through deriving target bioreactor properties from strain attributes, this new paradigm provides a reliable framework to estimate outdoor productivities from yields determined experimentally under low light.

Provided adequate agitation to sustain high yield biomass production, steady-state biomass production can be easily parameterized using the autotrophic yield. Achieving such a steady-state is key to maximizing productivity. The set of simple equations presented in this work, the validity of which hinges on vigorous mixing conditions under high irradiance, averts the complex control strategies detailed in the literature.

Algal lipid accumulation has been broadly documented under nitrogen limitation in growth arrested cultures. However, growth arrest lowers overall lipid productivity and can lead to erroneous productivity projections (Wilhelm and Jakob 2011; Rodolfi et al. 2009). The concept of light as a continuously fed substrate brings about a different understanding of such lipid accumulation. Namely, lipid accumulation corresponds to a photon flux excess with respect to the flux of nitrogen molecules taken up by the culture, which can be parameterized under steady-state (Sect. 5.3). Upon determination of the culture autotrophic and nitrogen yields under nutrient-replete conditions, the nitrogen flux is lowered gradually until lipid production is achieved—at the cost of a lowered overall dry-weight productivity. This chapter details the methodology to achieve continuous autotrophic lipid production.

2 Sustainable Algal Lipid Production: Current Achievements and Upcoming Prospects

2.1 Biomass and Lipid Production Estimates

Algal lipids have been widely promulgated as a precursor to renewable transportation biofuels. Stress-induced autotrophic lipid accumulation has been documented in many algal species (Rodolfi et al. 2009; Griffiths and Harrison 2009), including phosphate limitation in *Ankistrodesmus falcatus* (Kilham et al. 1997), silicon and nitrogen deficiency (Tornabene 1983; Sheehan et al. 1998; Shifrin and Chisholm 1981) and alkaline pH stress in *Chlorella* sp. (Guckert and Cooksey 1990). However, lipid accumulation under these stress conditions—on the order of 20–40 % on a dry weight (DW) basis—have invariably been associated with prolonged growth arrest or severe growth rate reduction (Reitan et al. 1994; Gressel 2008).

Table 1 Example increase in dry weight specific energy in nitrogen-limited algal cells

	Mass fraction[b]	
	N-rich	N-limited
Carbohydrates (15.7 kJ g_{DW}^{-1})[a]	0.52	0.35
Lipids (37.6 kJ g_{DW}^{-1})[a]	0.08	0.3
Proteins (16.7 kJ g_{DW}^{-1})[a]	0.4	0.35
DW specific energy (kJ g_{DW}^{-1})[c]	17.9	22.6

[a] Values from (Rebolloso-Fuentes et al. 2001)
[b] Representatitve values ((Holland et al. 2011) and unpublished data)
[c] DW specific energy ratio of N-rich to N-limited is 0.79

Reported outdoor algal biomass productivities are on the order of 20–40 g_{DW} m^{-2} d^{-1} (Capo et al. 1999; Lundquist et al. 2010) under nutrient-replete conditions for average yearly irradiances of 390 μE m^{-2} s^{-1} (such as in southern US latitudes). As an oft-neglected consequence, the corresponding upper bound of lipid productivity (16 g_{LIPIDS} m^{-2} d^{-1} or 7,400 gal $acre^{-1}yr^{-1}$ at a lipid density of 850 g L^{-1} and 40 % lipids) needs to be lowered to account for the duration of the culture maturation and growth arrest. Indeed, the sole requirement of a one-day nitrogen starvation period to achieve high lipid content in a culture growing at 40 g_{DW} m^{-2} d^{-1} would half the above lipid productivity upper bound estimate to 8 g_{LIPIDS} m^{-2} d^{-1}.

Upon nitrogen limitation and subsequent lipid accumulation, the cell specific energy increases due to the higher specific energy of lipids, which is illustrated in Table 1 with representative values of algal cell compositions. Assuming a constant photosynthetic efficiency despite mild stress, nitrogen-limited lipid productivity estimates from nitrogen-replete productivity data should reflect the difference in DW specific energy, and should therefore be multiplied by 0.79 for the example given in Table 1.

Measured quantum efficiencies of 0.102 g_C/mole photons in algae (Cleveland et al. 1989) correspond to an achievable productivity of 82 g_{DW} m^{-2} d^{-1}, assuming 50 % C on a dry weight basis (Kroon and Thoms 2006) and average yearly irradiances of 390 μE m^{-2} s^{-1}. Such two- to four- fold increase in large-scale algal biomass productivity may be achievable using the methodology and insights provided in this work. Furthermore, understanding algal metabolism in a way to achieve continuous lipid production at high biomass productivities would permit lipid productions on the order of 16 g_{LIPIDS} m^{-2} d^{-1} (25 % harvestable lipids from cells containing 30 % on a DW basis, at 390 μE m^{-2} s^{-1}, and corrected for higher specific energy content of lipid-rich cells as in Table 1) or 7,500 gal $acre^{-1}yr^{-1}$ (at a lipid density of 850 g L^{-1}). For comparison with crop-based agriculture, Malaysia palm oil productivity was 473 gal $acre^{-1}$ yr^{-1} in 2008 (Malaysian Palm Oil Industry Performance 2008 (Anon 2009), with a density of 890 g L^{-1}), which is 16-fold less than the projected algal lipid productivity.

2.2 Irradiance Unit Conversions

Energy calculations of achievable productivity depend on the measurement of incident light as a Photosynthesis Photon Flux Density (PPFD, in μE m^{-2} s^{-1}) in the PAR region between 400 nm and 700 nm. While quantum meters readily provide such measurements, outdoor light levels are commonly reported in W m^{-2} using a pyranometer. Unit conversions between photon flux and energy are derived using corresponding light source spectra.

Two geometries of sensors are commonly used in the field to measure incident light, either as energy per area or photon flux per area. The more common 2π half-sphere sensors measure light incident onto a surface, and the 4π full-sphere sensors measure light incident from all directions. The use of 4π sensors, which can give readings up to twice those of 2π sensors, is more relevant for bioreactors at an angle from the ground, whereas 2π sensors are more relevant for pond configurations. For complex reactor geometries, (Sánchez Mirón et al. 2000) used chemical actinometry to measure the precise incident PPFD. In our analysis below, we assume the use of 2π sensors to quantify direct normal-incident PPFD.

Solar radiation spectra are typically reported as a plot of photon energy $E_p(\lambda)$ (in W m^{-2} nm^{-1}) measured for each wavelength increment $d\lambda$ (ASTM 2003; Thuillier et al. 2003). The photon energy $E_p(\lambda)$ is proportional to the photon flux $\dot{n}(\lambda)$:

$$E_P(\lambda)d\lambda = \dot{n}(\lambda) \cdot Na \cdot \frac{hc}{\lambda} d\lambda \tag{1}$$

where h is Planck's constant in S.I. units; c the celerity of light in m s^{-1}; Na is Avogadro's constant in mol^{-1}; $E_p(\lambda)$ is the energy reported for each wavelength increment $d\lambda$ at λ in W m^{-2} nm^{-1}; $\dot{n}(\lambda)$ is the photon flux reported for each wavelength increment $d\lambda$ at λ in Einstein s^{-1} m^{-2} nm^{-1}. These solar spectra can thus be used to convert units of Einstein and Joules (c_{EJ} in units of E J^{-1}), with Einstein as the photon flux in the PAR region, and total energy measured in the wavelength range λ_1- λ_2:

$$c_{EJ} = \frac{\int_{400}^{700} \dot{n}(\lambda)d\lambda}{\int_{\lambda 1}^{\lambda 2} E_P(\lambda)d\lambda} = \frac{10^{-9}}{h \cdot c \cdot Na} \frac{\int_{400}^{700} \lambda \cdot E_P(\lambda)d\lambda}{\int_{\lambda 1}^{\lambda 2} E_P(\lambda)d\lambda} \tag{2}$$

Analogously, spectra measured in W m^{-2} nm^{-1} can be converted to a normalized photon flux frequency $P_{SUN}(\lambda)$ in nm^{-1} in the PAR region (Fig. 1):

$$P_{SUN}(\lambda) = \frac{\lambda \cdot E_P(\lambda)}{\int_{400}^{700} \lambda \cdot E_P(\lambda)d\lambda} \tag{3}$$

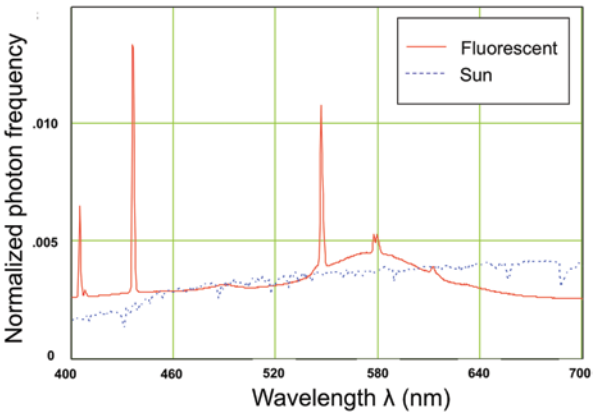

Fig. 1 Normalized photon frequency in the PAR region for the acquired fluorescent light spectrum and calculated for the ASTM ground direct-normal spectrum (Eq. 3)

The fraction of energy in the PAR region, given a total energy measured in the wavelength range λ_1–λ_2, is:

$$F_{PAR} = \frac{\int_{400}^{700} E_P(\lambda)d\lambda}{\int_{\lambda 1}^{\lambda 2} E_P(\lambda)d\lambda} \tag{4}$$

Percent energy in the PAR region as well as Einstein-to-Joules conversion factors are reported in Table 2. Outer space (Space) spectrum data was kindly provided by Dr. Thuillier (Thuillier et al. 2003). For ground irradiance, ASTM spectra (ASTM 2003) were used as reference ground spectra, for a 37° tilted surface (Tilted) and a direct-normal surface (Flat). The ASTM spectra are reported for an air-mass (AM) coefficient of 1.5, which provides a description on the relative light attenuation due to atmospheric water vapor concentration (Mecherikunnel et al. 1983), at conditions still conducive to photovoltaic applications (ASTM 2003). The wavelength ranges were chosen to reflect apparatus available commercially, such as a Li-Cor pyranometer, usually 400–1100 nm range, (Kania and Giacomelli 2001) or a Precision Spectral Pyranometer (PSP, 285–2800 nm range), used by the NREL (http://rredc.nrel.gov/solar/pubs/redbook/) for its solar radiation measurements.

Despite marked variations in the overall sun spectrum due to an air-mass coefficient AM of 1.5, the conversion factors and percent energy calculations do not vary significantly between ground and outer-space data (Table 2). This is likely due to the fact that the ground solar spectrum in the PAR region changes drastically in shape for AM >1.5 but not below (Mecherikunnel et al. 1983). These tabulated values provide an updated tool which should help prevent the use of erroneous conversion factors (Kania and Giacomelli 2001).

Table 2 Einstein-to-Joules conversion factors c_{EJ} and Percent energy in the PAR region. An outer space spectrum (Space), an ASTM 37° tilted ground spectrum (Tilted) and an ASTM ground direct-normal spectrum (Flat) were used

	c_{EJ} in μE J^{-1}			% Energy in the PAR region		
Ref. spectrum range	200–2400 nm	280–4000 nm		200–2400 nm	280–4000 nm	
Ref. spectrum	Space	Flat	Tilted	Space	Flat	Tilted
PAR (400–700 nm)	4.55	4.63	4.60	100	100	100
Li-Cor (400–1100 nm)	2.67	2.55	2.61	58.7	55.1	56.7
PSP (285–2800 nm)	1.84	1.95	1.99	40.5	42.0	43.3
Overall sun spectrum	1.83	1.93	1.98	40.2	41.6	43.0

As photosynthesis is known to occur in the near-UV range between 350 and 400 nm (Sakshaug and Johnsen 2006), the various reference spectra were used to calculate the % photon flux in the near-UV range compared to the flux in the 350–700 nm range (near UV+PAR). These values were 5.76% (Space), 3.94% (Flat) and 4.89% (Tilted), such that the near-UV contribution can be mostly neglected for outdoor level estimates.

Spectrometers allow for the acquisition of light source spectra in the PAR region, where the count reading $P(\lambda)$ in a given increment $d\lambda$ is proportional to the photon flux $\dot{n}(\lambda)$ by a constant β:

$$P(\lambda) = \beta \cdot \dot{n}(\lambda) = \frac{\beta}{h \cdot c \cdot Na} \cdot \frac{E_P(\lambda)}{\lambda} \tag{5}$$

These relative photon-count spectra can therefore be used to calculate c_{EJ} (in units of E J^{-1}) the conversion from Einstein to Joules (or E s^{-1} to W), as shown above, where both PPFD and energy are measured in the PAR region:

$$c_{EJ} = \frac{10^{-9}}{h \cdot c \cdot Na} \frac{\int_{400}^{700} P(\lambda) d\lambda}{\int_{400}^{700} \frac{P(\lambda)}{\lambda} d\lambda} \tag{6}$$

Two $P(\lambda)$ spectra for fluorescent light sources of different intensities were acquired using an Ocean Optics spectrometer (in the 400–700 nm range), in both cases resulting in calculated conversion factor c_{EJ}=4.49 μE J^{-1}. An incident PPFD of 50 μE m^{-2} s^{-1}, for example, provides a culture with an energy of 11.1 W m^{-2}.

2.3 Sustainability Considerations

Achieving sustainable biomass production from algae entails a comprehensive analysis of the overall process, for which all feedstocks and energy sources should be renewable. Hence, providing flue gas from coal fired plants as a CO_2 source

http://www.springer.com/978-94-007-7493-3

Algal Biorefineries
Volume 1: Cultivation of Cells and Products
Bajpai, R.K.; Prokop, A.; Zappi, M.E. (Eds.)
2014, XIII, 324 p. 62 illus., 34 illus. in color., Hardcover
ISBN: 978-94-007-7493-3